

STATISTICAL TEXTURE CLASSIFICATION VIA HISTOGRAMS OF WAVELET FILTERED IMAGES

ALAN WEE-CHUNG LIEW¹, JUN JO¹,
TAE BYONG CHAE² and YONG-SIK CHUN²

¹School of Information and Communication Technology,
Gold Coast campus, Griffith University, QLD4222, Australia
{a.liew@griffith.edu.au, j.jo@griffith.edu.au}

²Department of KOMPSAT-5 System Engineering & Integration
Korea Aerospace Research Institute
POB 113 Yusung Daejeon, 305-333, KOREA
{sik@kari.re.kr}

Abstract:

We show how the first order statistic, i.e. the histogram, of the wavelet filtered image is related to the higher order statistic of the original image. We then propose a texture classification method that uses the histogram information of the filtered images as the feature vector. Classification experiments show that the proposed method achieves better classification result than the Gabor wavelet filtering method using only the mean and standard deviation of the absolute filtered images as feature vectors.

Keywords:

Texture classification; wavelet filter; spatial grey level dependence

1. Introduction

Texture perception is an important part of vision since objects can often be distinguished by their characteristic textures despite their similarity in colors or shapes. With the advent of digital storage media, the use of textural information in performing content-based image retrieval from digital image library has become indispensable.

Most texture analysis methods can be categorized into either statistical approach or structural approach. The statistical approach attempts to use the statistical properties of the spatial distribution of grey level as texture descriptors. The structural approach, on the other hand, conceives of texture as an arrangement of a set of spatial sub-patterns or texture primitives according to some placement rules. Recently, wavelet filtering-based methods are being proposed for texture analysis and classification. In this paper, we discuss two well-known statistical texture classification methods, called the spatial grey level dependence (SGLD) method [1] and the wavelet filtering method [2, 6] and point out the underlying relationship

between these two methods. We then propose a new classification method that combine features from these two methods and give experimental results to illustrate its performance.

2. Texture Classification Methods

The SGLD method is based on the estimation of the second-order joint conditional probability distribution $p(i,j|d,\theta)$ where each $p(i,j|d,\theta)$ is the probability of going from the grey level i to the grey level j given the inter-sample distance d and the direction in angle θ . This method was inspired by the extensive psychovisual texture discrimination studies which showed human are sensitive to the second-order statistical variation in texture [5]. To characterize a texture adequately, a set of inter-sample distances and directions is generally used [1].

If the grey level range is quantized into N levels, then each (d_k, θ_k) will produce an $N \times N$ co-occurrence matrix. Instead of using these matrices directly, a number of parameters, e.g., angular second moment, contrast and entropy, are usually computed from each of these matrices and are used as texture descriptors. However, this inevitably reduces the discriminative power of the SGLD method. In addition, these parameters are usually proposed in an ad hoc manner and may be suboptimal.

In the wavelet filtering method, each wavelet filter at a particular orientation produces an output image with localized spectrum at different location in the frequency plane. The localized spatial-frequency resolution of the wavelet function allows a local analysis of the image at different frequency resolution. The mean μ and standard deviation σ of the absolute image are usually calculated from each of the output images and are used as texture

descriptors ([2] uses both μ and σ where as [6] uses only μ)

Since many image structures, i.e., directionality, periodicity, and coarseness, and their properties can be inferred from the local spectrum, the wavelet filtering method can produce meaningful texture descriptors describing these image structures. However, in attempting to characterize the local spectrum using only two parameters μ and σ , much useful information are lost. Moreover, unlike the SGLD method, this method does not appear to relate to the extensive psychovisual texture discrimination studies.

3. First Order Statistics of the Filtered Image

We focus our attention on the 1-D case for clarity of presentation although the analysis extends directly to 2-D. Let $\{h_n\}_{n=0, \dots, N-1}$ be the coefficients of an N-tap filter. For a discrete 1-D signal f of length L , the convolution of the filter and the signal can be written as

$$y_t = \sum_{n=0}^{N-1} h_n f_{t+n}, t = 0, \dots, L-1 \quad (1)$$

where we assume that the signal has been reflected about the origin. Let F and Y be the random variables associated with the input image and the filter output respectively. Clearly, the range of value for Y is dependent on the range of grey level value $R(F)$ of the input signal and the filter coefficients. The probability that Y assumes a particular value, say, y_i , is then given by

$$\begin{aligned} p(Y = y_i) &= p\left(\sum_{n=0}^{N-1} h_n f_n = y_i\right) \\ &= \sum_{f_0} \dots \sum_{f_{N-2}} p\left(f_0, f_1, \dots, f_{N-2}, \frac{1}{h_{N-1}}(y_i - h_0 f_0 \right. \\ &\quad \left. - h_1 f_1 - \dots - h_{N-2} f_{N-2})\right) \end{aligned} \quad (2)$$

where $\{f_0, f_1, \dots, f_{N-2}\} \in R(F)$. In terms of the N-order joint conditional probability,

$$\begin{aligned} p(Y = y_i) &= \sum_{f_0} \dots \sum_{f_{N-2}} p\left(f_0, f_1, \dots, f_{N-2}, \frac{1}{h_{N-1}}(y_i - h_0 f_0 \right. \\ &\quad \left. - h_1 f_1 - \dots - h_{N-2} f_{N-2}) | d_1 = d_2 = \dots \right. \\ &\quad \left. = d_{N-1} = 1\right) \end{aligned} \quad (3)$$

where the inter-sample distance d_k denotes the distance between sample $k-1$ and sample k . Note that the subscript of

f in (2) and (3) is not a time index but rather denotes the relative position of the elements in the signal vector f with respect to the filter coefficients. For $N = 2$, (3) becomes

$$p(Y = y_i) = \sum_{f_0} p\left(f_0, \frac{1}{h_1}(y_i - h_0 f_0) | d_1 = 1\right) \quad (4)$$

Let M be the co-occurrence matrix with elements $p(f_0, f_1 | d_1=1)$ and with the x and y-axis labeled by the random variables F_0 and F_1 respectively. Then (4) implies that the probability of the filter output $Y=y_i$ is given by the sum of the elements of the co-occurrence matrix M lying on the straight line with gradient given by h_0/h_1 ,

$$F_1 = \frac{y_i}{h_1} - \frac{h_0}{h_1} F_0 \quad (5)$$

Similarly, for $N=3$, the probability of $Y=y_i$ is given by the sum of the elements of a 3-D joint conditional probability matrix lying on the plane

$$F_2 = \frac{y_i}{h_2} - \frac{h_0}{h_2} F_0 - \frac{h_1}{h_2} F_1 \quad (6)$$

Thus, the first-order statistics, i.e., the histogram, of a signal filtered by a 2-tap filter provides a description (i.e. histogram of the sum of elements of M at parallel lines with gradient h_0/h_1) of the second-order statistics, i.e., the co-occurrence matrix, of the original signal. In general, given an N-tap filter with N non-zero filter coefficients, the first-order statistics of the filtered signal provides a description of the N-order statistics of the original signal. The filtering operation therefore produces a statistical simplification of the original signal. It should be noted that while the first-order statistics of the filtered signal can be obtained from the higher order statistics of the original signal, the converse is not true.

The above analysis shows how the filter outputs are related to the higher order statistics of the original image. So rather than trying to summarize the N-order statistics of the original image with simple statistics such as μ and σ , the complete histogram of the filtered image would provide better discriminating power. Although the above discussion is applicable to any filtering scheme, the wavelet filtering scheme does have some advantages. Firstly, the localized spatial-frequency support of the wavelet functions enables local analysis of texture elements. Secondly, the wavelet multiresolution framework allows texture to be analyzed at different resolution in a consistent manner.

4. Proposed Classification Method and Results

In the proposed method, a texture image is first filtered with a set of cortex wavelet filters [4] tuned to 4 orientations and 4 scales. A schematic of the spatial frequency plane division of this filter is shown in Fig. 1.

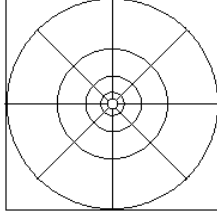


Fig. 1: Spatial frequency plane division of the cortex wavelet filters. The scales are in octave, orientation in 45° .

After filtering, the grey level cumulative density function (cdf) of each filtered image is computed and the grey levels corresponding to the $0.1k$ ($k=1$ to 10) probability of the cdf are used as the texture features. The features from the 16 filtered images, together with the features from the original image, the low-pass and high-pass residues which are obtained similarly, are concatenated to form the raw feature vector for the texture image.

We performed a classification experiment in which the task is to assign a test image to one of the known texture classes. We collected 35 512×512 images consisting of 33 classes from the Brodatz texture set [5]. Images of size 128×128 are extracted from these larger images and randomly rotated, and 10 images from each class are used for training while 30 images from each class are used for testing. Some of the test images are shown in Fig. 2.

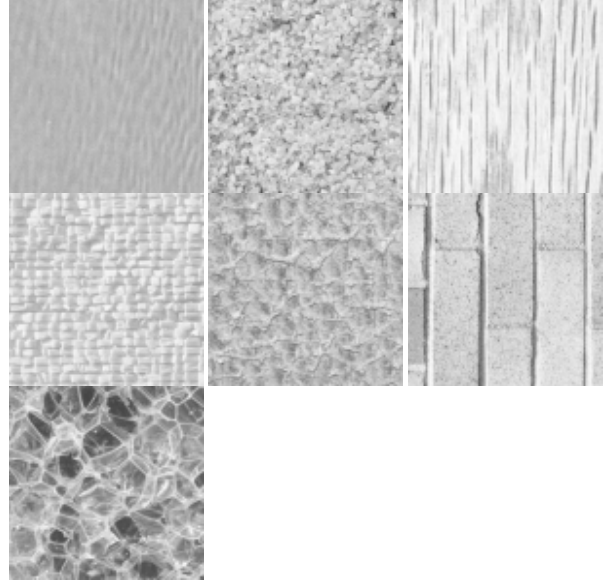
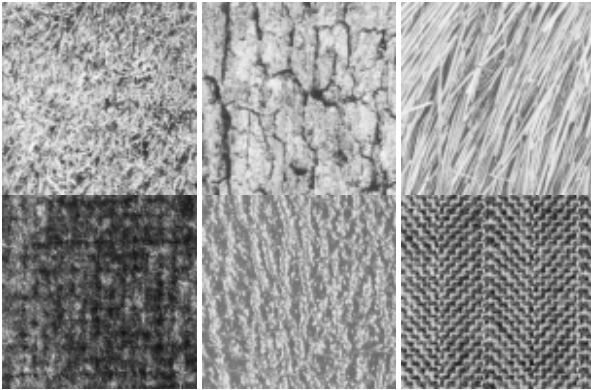


Fig. 2: Some test images obtained from [7]. Left to right, top to bottom: Grass, Bark, Straw, Woolen cloth, Herringbone weave, Pressed calf leather, Beach sand, Water, Wood grain, Raffia, Pigskin, Brick wall, Plastic bubbles.

For the training phase, the raw feature vector for each training image is first computed. The raw feature vectors then undergo Principle Component Analysis (PCA) followed by Linear Discriminant Analysis (LDA) [3]. During PCA, only the 80 most significant elements of the feature vector corresponding to the 80 largest eigenvalues are kept. At the LDA stage, the length of the feature vector is further reduced to 10. Finally, the class centroids are computed from the feature vectors.

During testing, the feature vector of the test image is projected onto the PCA and LDA spaces using the projection matrices obtained at the training phase. The resulting feature vector x is then compared to the class centroid c_i using the following distance metric,

$$d(x, c_i) = \sum_{j=1}^{10} \left(\frac{x(j) - c_i(j)}{\sigma(c_i(j))} \right)^2 \quad (7)$$

where $\sigma(c_i(j))$ is the standard deviation of the j th element in the class centroid c_i of class i . For comparison, we also performed the classification experiment using the Gabor wavelet filtering method as in [2]. Let the Gabor wavelet transform of an image $I(x, y)$ be given by

$$W_{mn}(x, y) = \int I(x_l, y_l) g_{mn}(x - x_l, y - y_l) dx_l dy_l \quad (8)$$

where g_{mn} is the Gabor wavelet at scale m and orientation

n . The μ_{mn} and σ_{mn} is given by

$$\mu_{mn} = \iint |W_{mn}(x, y)| dx dy \quad (9)$$

$$\sigma_{mn} = \sqrt{\iint (|W_{mn}(x, y)| - \mu_{m,n})^2 dx dy} \quad (10)$$

In [2], m and n are chosen to be 4 and 6, respectively, giving a total of 24 filtered images. This gives a feature vector of length 48. To allow a direct comparison, the Gabor texture feature vectors also undergo PCA and LDA to give a final length of 10 and use the same distance metric as in (7). Table 1 presents the average classification performance of each class for both methods. The overall average classification performance of our approach and Gabor approach are 98.4% with standard deviation of 3.9 and 92.8% with standard deviation of 9.6 respectively. Thus, with a smaller standard deviation, our approach is more robust and reliable.

5. Conclusions

We presented the theoretical basis for using the histograms of the wavelet filtered images as texture descriptor and showed its relationship to the spatial grey level dependence matrix when the number of filter tap equals to 2. Experimental results and comparison with the well known wavelet based texture classification method of Manjunath [2] have shown the feasibility and robustness of our approach. The histogram of the wavelet filtered images is able to provide rich description that better characterizes the texture than the simple mean and standard deviation of the absolute image. The method developed can be used to perform image region segmentation.

Acknowledgment

This work is supported by Korean Aerospace Research Institute.

References

- [1] R.M. Haralick, K. Shanmugam, and I. Dinstein, "Textural features for image classification", IEEE Trans. Systems Man and Cybernetics, Vol. 3, No. 6, pp. 610-621, Nov. 1973.
- [2] B.S. Manjunath, and W.Y. Ma, "Texture features for browsing and retrieval of image data", IEEE Trans. Pattern Analysis and Machine Intelligent, Vol. 18, No. 8, pp. 837-842, Aug 1996.

- [3] D.L. Swets, and J. Weng, "Using discriminant eigenfeatures for image retrieval", IEEE Trans. Pattern Analysis and Machine Intelligent, Vol. 18, No. 8, pp. 831-836, Aug 1996
- [4] A.B. Watson, "The cortex transform: Rapid computation of simulated neural images", Computer Vision, Graphics, and Image Processing, Vol. 39, pp. 311-327, 1987.
- [5] P. Brodatz, "Textures: A Photographic Album for Artists and Designers", New York: Dover, New York, 1966.
- [6] T. Chang and C.-C.J. Kuo, "Texture Analysis and Classification with Tree-Structured Wavelet Transform", IEEE Trans. Image Processing, vol. 2, no. 4, pp. 429-441, Oct. 1993.
- [7] <http://sipi.usc.edu/database/database.cgi?volume=textures>

TABLE 1. AVERAGE CLASSIFICATION PERFORMANCE (%)

Class	Our method	Gabor filtering
1	100	93.3
2	100	100
3	100	100
4	100	100
5	100	51.7
6	96.7	86.7
7	100	100
8	100	96.7
9	100	96.7
10	100	100
11	100	93.3
12	100	100
13	100	96.7
14	100	100
15	96.7	86.7
16	93.3	100
17	100	86.7
18	96.7	96.7
19	100	100
20	96.7	76.7
21	100	90
22	100	90
23	100	100
24	100	100
25	93.3	93.3
26	80	83.3
27	100	100
28	100	96.7
29	100	93.3
30	100	100
31	100	100
32	93.3	100
33	100	86.7
Average	98.4 (s.d=3.9)	92.8 (s.d=9.6)